

***Calendula officinalis*-mediated biosynthesis of Silver Nanoparticles and their Electrochemical and Optical Characterization**

Maged El-Kemary¹, Eslam Ibrahim², Mohammad, F. A-Ajmi³, Shaden A.M. Khalifa^{4,5}, Alanazi, A. D⁶., Hesham R. El-Seedi^{2,7,8,*}

¹Division of Photo- and Nanochemistry, Chemistry Department, Faculty of Science, Kafrelsheikh University, 33516 Kafr ElSheikh, Egypt.

²Department of Chemistry, Faculty of Science, El-Menoufia University, 32512 Shebin El-Kom, Egypt.

³Department of Pharmacognosy, College of Pharmacy, King Saud University, Riyadh 11451, P.O. Box 2457, Saudi Arabia.

⁴Department of Experimental Hematology, Karolinska University Hospital, SE-141 86 Stockholm, Sweden.

⁵Department of Molecular Biosciences, Stockholm University, the Wenner-Gren Institute, SE-106 91 Stockholm, Sweden.

⁶College of Applied Medical Sciences, Shaqra University, KSA, Aldawadmi 11911, P.O.Box 1678, Saudi Arabia.

⁷Division of Pharmacognosy, Department of Medicinal Chemistry, Uppsala University, Box 574, SE-75 123, Uppsala, Sweden.

⁸Department of Chemistry, Faculty of Science, University of Malaya, 50603 Kuala Lumpur, Malaysia.

*E-mail: hesham.el-seedi@fkog.uu.se

Received: 24 January 2016 / Accepted: 21 October 2016 / Published: 10 November 2016

The metal nanoparticles synthesis is highly explored field of nanotechnology. The biological methods seem to be more effective. A simple and elegant method is adopted to prepare Silver nanoparticles (AgNPs) in a single step using *Calendula officinalis* extract (COE) as reducing and stabilizing agent. The plant extract is mixed with AgNO₃ to get biosynthesized AgNPs. The biosynthesized AgNPs were both optically and electrochemically characterized by UV–Vis, Infrared spectroscopy, Transmission Electron Microscopy, Fluorescence spectroscopy, Zeta potential and Cyclic Voltammetry. The results showed *Calendula officinalis* extract is a useful bioreductant for the synthesis of AgNPs. This study infers that the size of biosynthesized AgNPs ranges from 30 to 50 nm. The surface plasmon resonance peak in the UV-Vis absorption spectra shows maximum absorption at 435 nm. Fluorescence spectra of silver nanoparticles, which show an emission peak at ~468 nm have also been studied. Zeta potential analysis ensured the biosynthesized AgNPs are highly stable. Using this environmentally friendly method of biological AgNPs production supplies rates of biosynthesis facile in comparison with other chemical and engineered routes. The employment of traditional medicine in biosynthesis protocols can

potentially open new doors in various human health and well-being implications such as cosmetics, foods and medicine.

Keywords: silver nanoparticles (AgNPs), biosynthesis, *Calendula officinalis* extract.

1. INTRODUCTION

Potential medical and pharmaceutical innovations have spurred investigation of nanotechnology [1]. The successful applications in the areas of sensors, electronics, optics among others typically renew the interest in developing techniques to produce drug carriers/particles based on nano-sized scale [2,3]. However, originally there was considerable doubt whether the minimum change of the particle shape and size can affect their physico-chemical properties. Progress in the past decade has revealed that the atomic and molecular aggregation of the nanoparticles have obvious effective physico-chemical criteria compared to their original bulk materials [4-8]. The vigorous ability to fabricate nanoparticles owes to a series of reactions produced by natural, incidental and engineered means. Recent evidence suggests that the natural pathway triggered by the environmental factors such as volcanic, lunar and mineral deposits and the process is as old as the earth's history itself. On the other hand, the man-made incidental pathway was resulted from the industrial pollution including welding fumes, diesel exhaust, coal combustion, forming anthropogenic particles. However, towards the made of engineered nanoparticles, four categories of fabrication were recommended [9,10] where carbon, metal, dendrimers and composite-based reactions are the main display.

Metal-based reactions, in particular, can follow different strategies; namely, reduction in solutions [11], biological reduction method [12], thermal decomposition [13], microwave [14], and laser mediated synthesis [15]. Biological reduction is done in the same manner as in other ways, although it is cheaper, easier, faster and eco-friendly. Various approaches using plant extract have been used for the synthesis of metal nanoparticles. Even when microbial, chemical and physical syntheses provide biological reduction; plant biosynthesis makes it possible to avoid the chemicals hazardous, waste, cell culture maintenance and the need of high-energy [16-25]. Plants are sufficient to induce wide-range of metabolites (e.g. enzymes, proteins, amino acids, vitamins, polysaccharides, and organic acids such as citrates secondary metabolites) that contribute to the biosynthesis of metal nanoparticles. Under the adequate circumstances, the noble metals i.e., gold (Au), platinum (Pt) and silver (Ag), are potent candidates for fabrication of nanoparticles [26-29].

Plants extracts and their counterparts of biomolecules play an important in both reducing and capping systems. These findings suggest that the plant extract composition and substrate concentration change the nanoparticles geometry and morphology, which can be triggered by a slight alteration of the size, shape or chemical composition of the nanoparticles [30-36]. Additionally, the introduction of plants to nanoparticles provides a safe arena for the bioreduction as for the wide distribution, availability and the feasibility of plants as to use on large scale. Several plants have been successfully used for efficient and rapid extracellular synthesis of silver nanoparticles such as leaf extracts of *Pelargonium graveolens*, *Azadirachta indica*, *Cymbopogon flexuosus*, *Tamarindus indica*, *Aloe Vera*,

Coriandrum sativum, *Cinnamomum camphora*, *Capsicum annuum*, *Gliricidia sepium*, *Pongamia pinnata*, *Datura metel*, latex of *Jatropha curcas*, *Zingiber officinale*, *Cinnamon zeylanicum* bark extract, *Eclipta* leaf, *Cycas* Leaf, *Hibiscus rosa sinensis*, *Terminalia chebula*, *Camellia Sinensis* and Orange peel extract [37] and references in there. *C. officinalis* is a plant in the genus *Calendula* of the family Asteraceae. Popular herbal and cosmetic products named 'calendula' invariably derive from *C. officinalis*. In this paper, we are the first who discuss the interaction between the silver nitrate and *C. officinalis* extract to form nanoparticles and provide the electrochemical and optical support of the biosynthesis.

2. EXPERIMENTAL

2.1. Materials

Silver nitrate (AgNO_3 ; 99.8%) was purchased from Cambrian Chemicals. Phosphate buffer solution (PBS) 0.1 M was prepared by addition 3.1 g of $\text{NaH}_2\text{PO}_4 \cdot \text{H}_2\text{O}$ and 10.9 g of Na_2HPO_4 (anhydrous) to distilled H_2O to make a volume of 1 L. The pH of the final solution will be 7.4. This buffer solution can be stored for up to one month at 4°C and can be used as supporting electrolyte. Ethanol used for extraction was purchased from Sigma-Aldrich. Aqueous solutions were prepared using double distilled water.

2.2. Preparation of leaf extract

The plant was collected and identified by Egyptian Agricultural Research Center, washed several times to remove the dust. The plant was then kept for sun drying. After sun drying, the plant material was finely powdered using a kitchen blender. For preparation of *C. officinalis* extract 3 g of powder was taken and mixed with 200 ml of Milli Q water and 100 ml ethanol, then kept in a water bath at 60°C for 70 min. The mixture was subsequently filtered through filter paper (Whatman No.42), to remove the insoluble plant biomass, giving a clear pale yellow color solution. The filtrate was stored in a refrigerator at 4°C for further studies.

2.3. Biosynthesis of silver nanoparticles

For the biosynthesis of AgNPs, 10 ml of the previously prepared COE is mixed with 100 ml of AgNO_3 solution (1 mM). Followed by heating the mixture in an oil bath at 70°C for 90 minutes.

2.4. Apparatus

Ultraviolet Visible (UV-Vis) Spectroscopy measurements were performed using a UV-2450 UV-Vis spectrophotometer (Shimadzu). Specimens for Transmission Electron Microscope (TEM)

were prepared by placing a drop of AgNPs on carbon-coated copper grids. TEM images were obtained using a JEM-2100 (JEOL) electron microscope. The Zeta potential analysis of purified silver nanoparticles dispersed in deionized water was performed to define the stability of biosynthesized AgNPs using Zeta PALs, Zeta potential analyzer (Brookhaven). Small quantity of very diluted solution of biosynthesized AgNPs (its absorbance less than 0.5) was taken in a transmission quartz cuvette for recording the emission spectrum (400–600 nm) of formed AgNPs using RF-5301 PC Spectrophotometer (Shimadzu). Fourier transform infrared (FT-IR) is used to detect the groups responsible for biosynthesis and stabilization of AgNPs by using FT-IR spectroscopy (IR100/IR 200 Spectrometer, USA). Cyclic voltammetry (CV) measurements were performed in analytical system model MF-9002 BASi Epsilon. Electrochemical experiments were carried out in a 20 mL voltammetric cell by using a three-electrodes configuration, at room temperature 27 °C. Glassy carbon electrode (GC, diameter 2 mm²) as working electrode, silver/silver chloride (Ag/AgCl) as reference electrode and platinum wire (Pt) as auxiliary electrode. The measurements were carried out in 10 mM phosphate buffer (pH 7.4). The potential was scanned from -1.0 to +1.0 V (versus Ag/AgCl) and then reversed to -1.0 V. The scan rate was 100 mV/s.

3. RESULTS AND DISCUSSION

3.1. UV–Vis studies

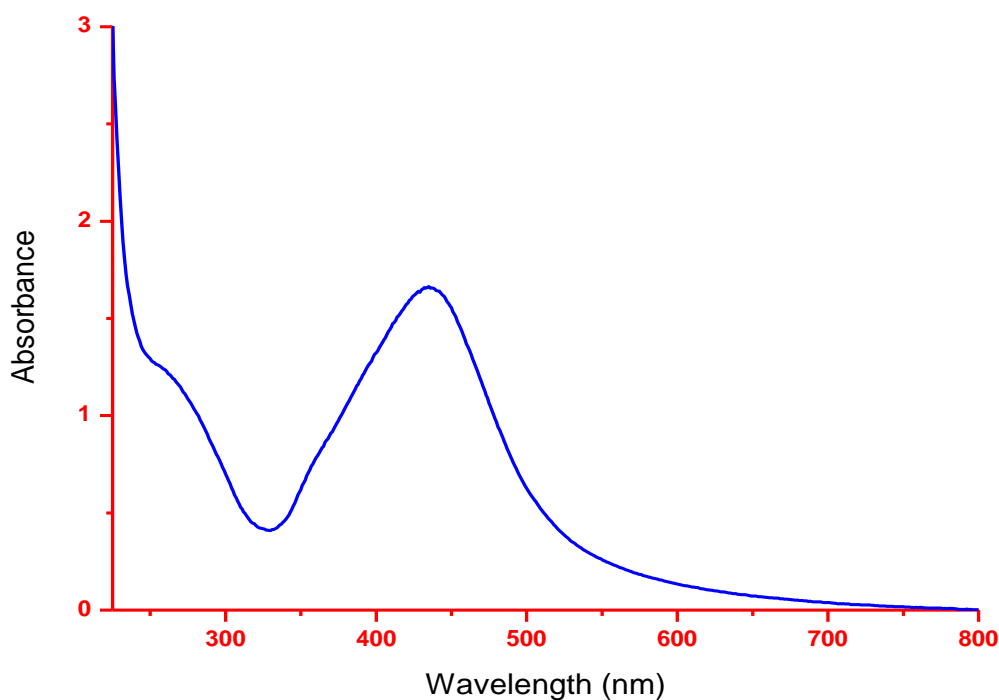


Figure 1. UV-visible absorption spectra of biosynthesized AgNPs

The biosynthesis of AgNPs was followed visually as the reaction color developed from pale yellow, light brown and ending with dark brown. Figure 1 shows the UV-vis absorption spectrum of the sample, showing the surface plasmon absorption of these Ag(0) particles, with absorption maxima ~ 435 nm. The excitation and emission of surface Plasmon vibrations at these fluorescent bands were used earlier as a landmark of silver nanoparticles characterization [38]. Raveendran et al. also observed a similar behavior [39].

3.2. Transmission electron microscopy

Figure 2 shows a typical transmission electron microscope (TEM) images. A size range of 30 to 50 nm was shown and found within a capping layer of 3-5 nm thick (Fig. 2b). The AgNPs crystallization was detected and typical SAD pattern was justified by the selected area diffraction (SAD) (Fig. 2c). Measurement of the electron diffraction on a number of crystals resulted in a ring pattern decorated with discrete spots.

An evident that is consistent with our findings that the majority of the particles exists as individual crystals and mainly attracted to the Ag core attributing to the main fcc silver crystal lattice.

3.3. Fourier Transform infra-red (FTIR) spectroscopy studies

The suspension of nanoparticles was found to be stable for a long period of time exceeded 8 months, which shows that these nanoparticles were stabilized in solution by the biomolecules present in plant extract. The stability of the as synthesized silver nanoparticles was confirmed by carrying out the FT-IR measurements on these samples. Fig. 3 shows the FT-IR spectra of silver nanoparticles. A weak band appears around 3496 cm^{-1} may be due to the stretching frequency of the O-H bond possibly arising from the carbohydrates or proteins present in the sample. The band at 3284 cm^{-1} may be assigned to N-H stretching of the primary amide $-\text{NH}_2$ group, which possibly arise from proteins. Where the weak band appeared at 2380 cm^{-1} might be attributed to the existence of charged amines (C-NH^+) [37]. The bands at 1657 cm^{-1} is due to C=O stretching mode of amide groups in the protein molecules. The weak band appears at 1253 cm^{-1} may be due to C-N stretching of the amide residue. A strong peak at 583 cm^{-1} could be determined as the metal-ligand stretching frequency appearing by virtue of the interaction of biomolecules to the AgNPs surfaces [40]. These observed peaks in this FT-IR spectra of biosynthesized AgNPs are exhibiting the existence of the biomolecules such as proteins which interact with nanoparticle surface. Consequently, protein molecules present in COE are playing a vital role in reducing, capping and stabilization of biosynthesized AgNPs [41, 42]. From earlier studies, it is known that proteins can bind to AgNPs via free amine groups in the proteins [43] so that, stabilization of the biosynthesized AgNPs by surface-bound proteins by means of covering AgNPs and acting as a stabilizing agent to prevent their agglomeration. [44].

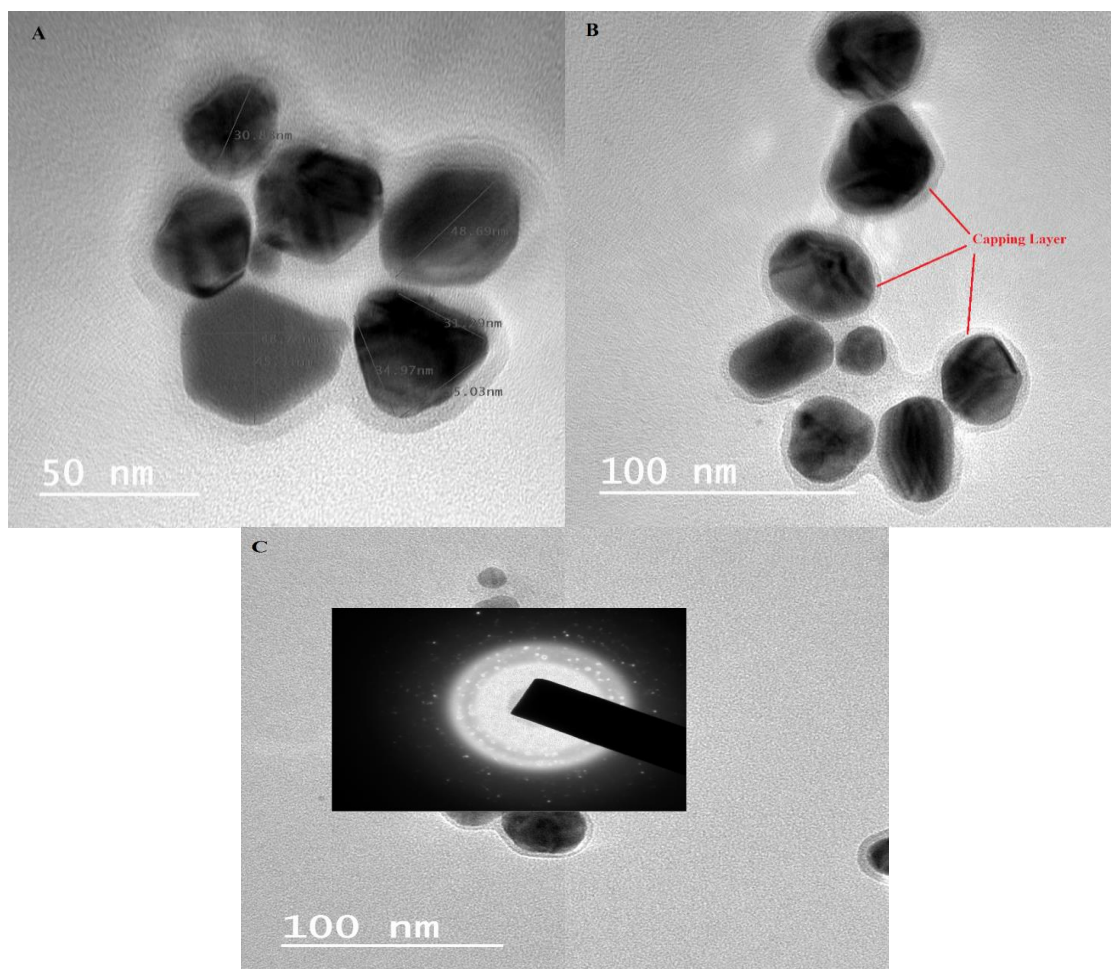


Figure 2. TEM images of biosynthesized AgNPs showing (a. the size ranges from 30 to 50 nm b. the capping layer around the AgNPs c. diffraction pattern of biosynthesized AgNPs)

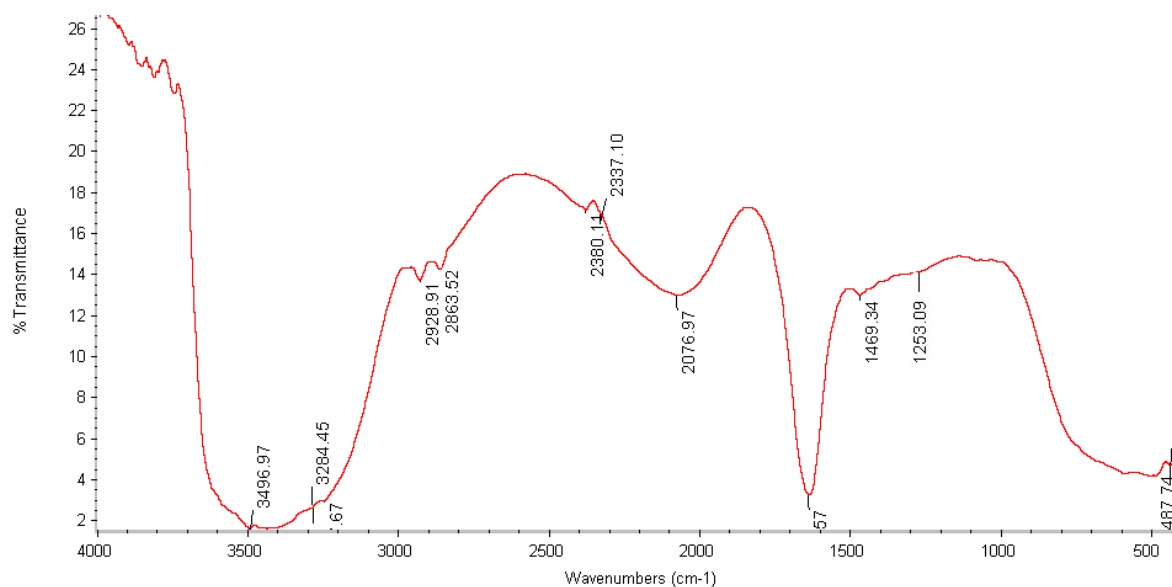


Figure 3. FT-IR spectrum of biosynthesized AgNPs showing possible functional groups responsible for bioreduction and stabilization of AgNPs.

3.4. Fluorescence spectroscopy

Figure 4 shows the fluorescence emission spectra of the AgNPs dispersed in water upon excitation at 400 nm. The maximum fluorescence emission peak was observed at ~ 468 nm. Jian et al., have reported a similar fluorescence emission peak at 470 nm for AgNPs. The origin of this peak is probably due to local field enhancement [45]. However, A. Mooradian attributed the observed fluorescence from noble metals to transitions of electrons in the band below the Fermi level to holes in the d bands [46]. Also, fluorescence from Au nanoparticles has been attributed to interband electronic transition between the $6sp^1$ conduction band and $5d^{10}$ valence levels [47].

3.5. Zeta potential analysis

The general dividing line between stable and unstable suspensions is usually taken at either +30 or -30 mV. Particles with zeta potentials positive than +30 mV or negative than -30 mV are usually considered stable. Zeta potential more positive than -15 mV indicates suspension at the threshold of agglomeration [37]. Zeta potential measured for the AgNPs in the present study is -27 (mV) (Fig. 5). The -25 mV high zeta potential ensured the stabilization of the metal nanoparticles by making a high-energy barrier [48]. It was also suggested that the existence of these negatively charged electrostatic repulsive forces possibly maintain the metal nanoparticles without tending to aggregation [49].

3.6. Cyclic voltammetry analysis

In general, terms cyclic voltammetry (CVs) takes the potentiodynamic electrochemical measurements to further level beyond the definite potential. Two factors are predominantly used to define the critical values of the cyclic voltammetry and they are the set potential, the electrode's potential ramp. It is important to plot the working electrode versus the applied voltage. An alteration of the cyclic voltammogram indicates the significant electrochemical threshold of an analyte in solution where the inversion can undergo several times within the same experimental set. The cyclic voltammetry plateau was derived from prominent anodic and cathodic peaks (fig. 6) at a rate of 100 mV/s in phosphate buffer solution. Compton's group demonstrated theoretically and experimentally that stripping potential of AgNPs depends on the size of the particles [50]. The anodic peak has superior potential ascribed to the oxidation of AgNPs the raise of the cathodic peak is related to the reduction of the particles. The sharpness of the plateau requires a fast biosynthesis reaction in contrast to the decline of the peaks that was constantly indicated in correspondence to the diffusion/concentration ratio. Whilst the photochemical and physical properties highlighted the formation of AgNPs, the accompanied oscillation of the electrochemical dissolution/stripping between +440 mV and +111 mV at the voltammogram cycle. Here we can see that for the consecutive cycles the corresponding reduction and oxidation peaks of AgNPs were clearly increasing. It implies that the AgNPs were electrodeposited at the GC electrode surface [51,52]. We could find our results could be documented largely in comparison to that earlier studies come in [53]. Also Giovanni and Pumera

investigated the electrochemical behavior of silver nanoparticles of sizes 10-107 nm and they got data which ours are very similar to [54].

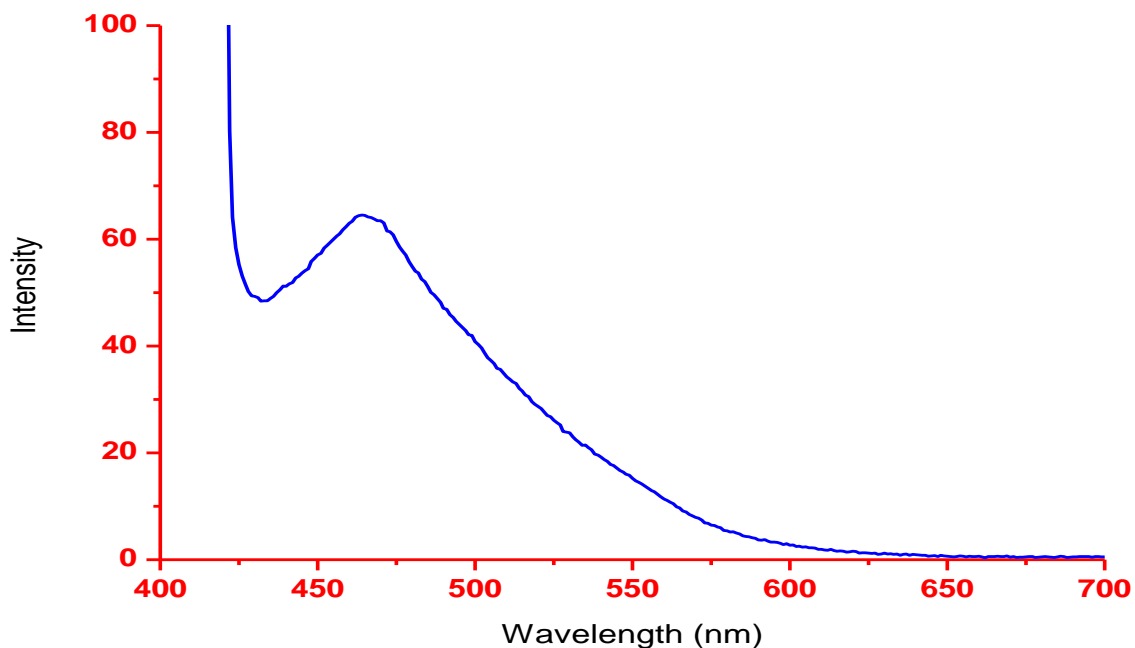


Figure 4. Fluorescence spectra of the biosynthesized AgNPs upon excitation at 400 nm in double distilled water.

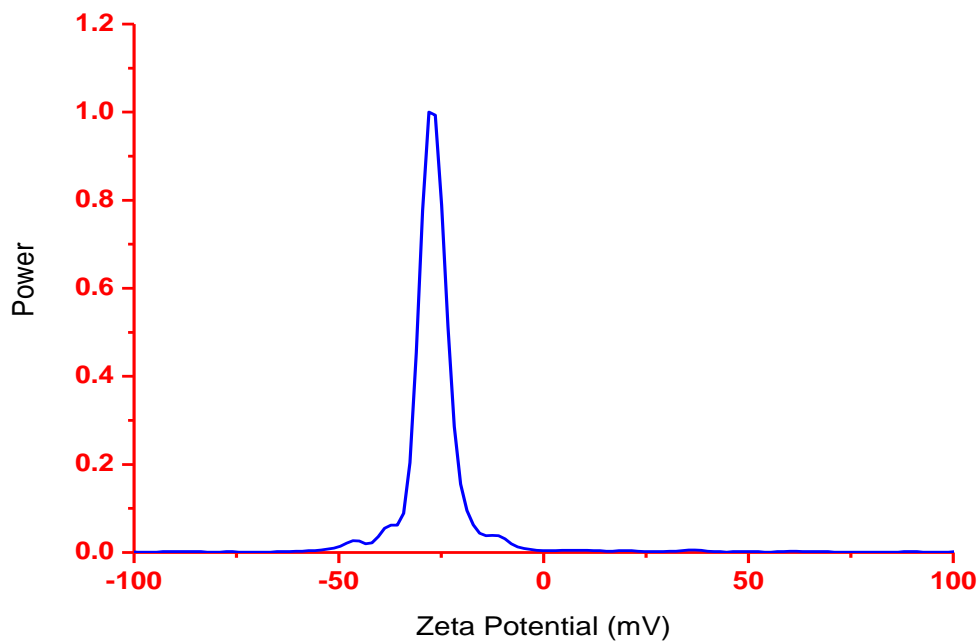


Figure 5. Zeta potential study of the biosynthesized AgNPs.

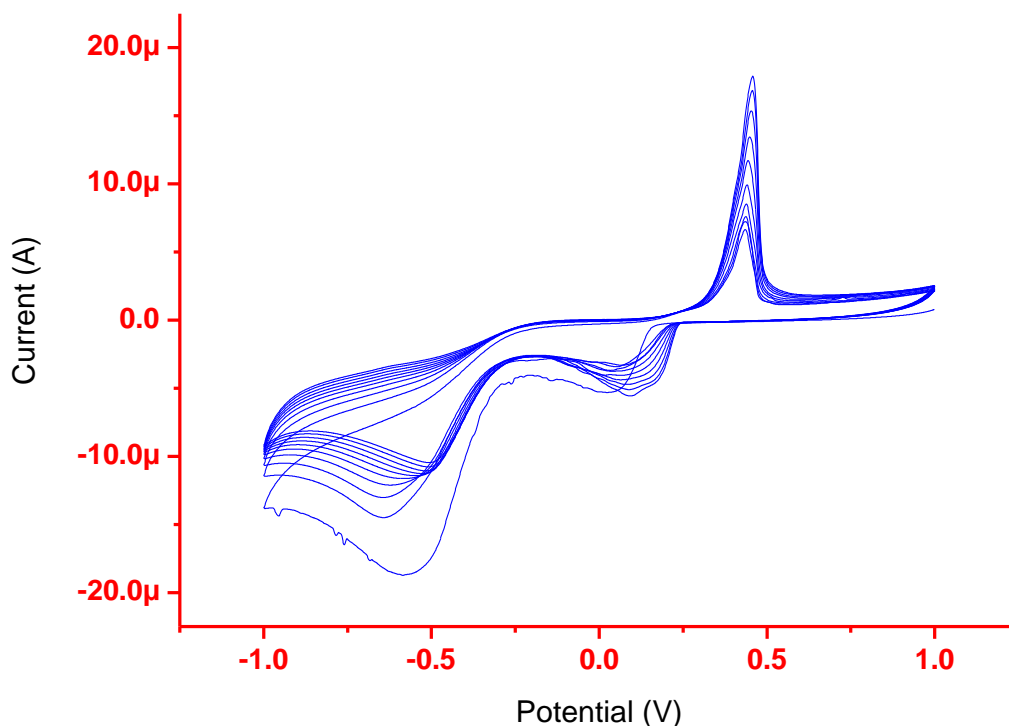


Figure 6. Multiple scan CV of biosynthesized AgNPs using *C. officinalis* extract

4. CONCLUSIONS

A variety of biosynthetic metal particles are now available for simple and rapid scale-up of medical and pharmaceutical dependent applications. Our scope of work was to carry out the biosynthesis of silver nanoparticles using *C. officinalis* extract and conduct physical, electrochemical and optical investigations. When considering optimizing the bioreduction mechanism, there is a whole range of parameters to take into account. These include the shape, size, surface area, crystallinity and efficacy among others. A selected group of advanced strategies along with a brief summary of their potential yields were listed in this report. In brief, the color replenished from pale yellow to dark brown meaning the binding of the extract with silver nitrate and forming the building blocks of the nanoparticles. The recognition of the silver nanoparticles was confirmed further by UV-vis spectroscopy TEM, Fluorescence spectroscopy, FT-IR, Zeta potential and CVs. Semi spherical and monodisperse AgNPs with the size ranging from 30 to 50 nm are biosynthesized successfully. Surface plasmon resonance peak is detected at 435 nm is detected by UV-VIS Spectrophotometer while fluorescence emission peak is clearly observed using Spectrofluorophotometer at 486 nm. Spectroscopic study expected that protein molecules present in plant extract are playing a vital role in reducing, capping and stabilization of biosynthesized silver nanoparticles, this deriving enhanced by appearing a capping layer of 3-5 nm thick around the biosynthesized AgNPs. Zeta potential measurements showed that the biosynthesized AgNPs are highly stable owing to existence of

negatively charged electrostatic repulsive forces possibly maintain the AgNPs without tending to accumulation. CVs studies revealed a higher current peak as 18 μ A at +440 mV.

ACKNOWLEDGEMENT:

We are very grateful to the generous support provided by deanship of research, King Saud University under research group number RGP-150.

References

1. J.A. Dahl, B.L.S. Maddux and J.E. Hutchison, *Chem. Rev.*, 107 (2007) 2228-2269.
2. D.S. Tiwari and Q.Z. Dunn, *J. Mater. Sci.*, 44 (2009) 5063-5079.
3. A.S. Maybodi, S.K.N. Darzi and R. Akhoondi, *Int. Nano Lett.*, 1 (2011) 52-58.
4. A. Biffis, N. Orlandi and B. Corain, *Adv. Mater.*, 15 (2003) 1551-1555.
5. M.C. Roco, *J. Nanopart. Res.*, 5 (2003) 181-189.
6. P.M. Tessier, O.D. Velev, A.T. Kalambur, J.F. Rabolt, A.M. Lenhoff and E.W. Kaler, *J. Am. Chem. Soc.*, 122 (2000) 9554-9555.
7. A. Nel, T. Xia, L. Mädler and N. Li, *Science*, 311 (2006) 622-627.
8. T.J. Brunner, P. Wick, P. Manser, P. Spohn, R.N. Grass, L.K. Limbach, A. Bruinink and W.J. Stark, *Environ. Sci. Technol.*, 40 (2006) 4374-4381.
9. D. Lin and B. Xing, *Environ. Pollut.*, 150 (2007) 243-250.
10. Y. Yu-Nam and R. Lead, *Sci. Total Environ.*, 400 (2008) 396-414.
11. E.A. Terenteva, V.V. Apyari, S.G. Dmitrienko and Y.A. Zolotov, *Spectrochim. Acta Part A*, 151 (2015) 89-95.
12. M. Sastry, A. Ahmad, M.I. Khan and R. Kumar, *Curr. Sci.*, 85 (2003) 162-170.
13. S. Navaladian, B. Viswanathan, R. P. Viswanath and T. K. Varadarajan, *Nanoscale Res. Lett.*, 2 (2007) 44-48.
14. A.M. Shanmugaraj and S.H. Ryu, *Electrochim. Acta*, 74 (2012) 207-214.
15. R. Zamiri, A. Zakaria and H. Abbastabar, *Int. J. Nanomedicine*, 6 (2011) 565-568.
16. Y.C. Liu and L.H. Lin, *Electrochem. Commun.*, 6 (2004) 78-86.
17. S.A. Vorobyova, A.I. Lesnikovich and N.S. Sobal, *Colloids Surf. A*, 152 (1999) 375-379.
18. C.H. Bae, S.H. Nam and S.M. Park, *Appl. Surf. Sci.*, 197 (2002) 628-634.
19. D. Mandal, M.E. Blonder, D. Mukhopadhyay, G. Sankar and P. Mukherjea, *Appl. Microbiol. Biotechnol.*, 69 (2000) 485-492.
20. S. Basavaraja, D.F. Balaji, A. Lagashetty, A.H. Rajasab and A. Venkataraman, *Mater. Res. Bull.*, 43 (2008) 1164-1170.
21. A.P. Kulkarni, A.A. Srivastava and R.S. Zunjarrao, *Int. J. Pharm. Bio. Sci.*, 3(2012) 121-127.
22. S. Keki, J. Torok and G. Deak, *J. Colloid Interface Sci.*, 229 (2000) 550-553
23. A.K. Jha and K. Prasad, *Int. J. Green Nanotechnol. Phys. Chem.*, 1 (2010) 110-117
24. D.G. Yu, *Colloids Surf. B*, 59 (2007) 171-178
25. S. He, Z. Guo, Y. Zhang, S. Zhang, J. Wang and N. Gu, *Mater. Lett.*, 61 (2007) 3984-3987.
26. C.B. Murray, S. Sun, H. Doyle and T. Betley, *MRS Bull.*, 26 (2001) 985-991.
27. R. Murray, S. Rosenthal, S. Kobayashi and A. Pfaller, *Medical Microbiology*, Mosby, Saint Louis (1998).
28. J. Dai and M.L. Bruening, *Nano. Lett.*, 2 (2001) 497-501.
29. M. Okuda, Y. Kobayashi, K. Suzuki, K. Sonoda, T. Kondoh, A. Wagawa, A. Kondo and H. Yoshimura, *Nano. Lett.*, 5 (2005) 991-993.
30. G. Schmid (Ed.), *Nanoparticles: From Theory to Application*, Wiley-VCH, Weinheim (2004).
31. R. Arunachalam, S. Dhanasingh, B. Kalimuthu, M. Uthirappan, C. Rose and A.B. Mandal, *Colloids Surf. B*, 94 (2012) 226-230.

32. Y. Yagci, O. Sahin, T. Ozturk, S. Marchi, S. Grassini and M. Sangermano, *React. Funct. Polym.*, 71 (2011) 857-862.
33. X. Wei, M. Luo, W. Li, L. Yang, X. Liang, L. Xu, P. Kong and H. Liu, *Bioresour. Technol.*, 103 (2012) 273-278.
34. M. Rai, A. Yadav and A. Gade, *Crit. Rev. Biotechnol.*, 28 (2008) 277-284.
35. N. Duran, P.D. Marcato, M. Duran, A. Yadav, A. Gade and M. Rai, *Appl. Microbiol. Biotechnol.*, 90 (2011) 1609-1624.
36. N. Mokhtari, S. Daneshpajouh, S. Seyedbagheri, R. Atashdehghan, S. Abdi K Sarkar, S. Minaian, H.R. Shaverdi and A.R. Shaverdi, *Mater. Res. Bull.*, 44 (2009) 1415-1421.
37. R.W. Raut, V.D. Mendhulkar and S.B. Kashid, *J. Photochem. Photobiol. B*, 132 (2014) 45-55.
38. R.W. Raut, N.S. Kolekar, J.R. Lakkakula, V.D. Mendhulkar and S.B. Kashid, *Nano-Micro Lett.*, 2 (2010) 106-113.
39. P. Raveendran, J. Fu and S.L. Wallen, *J. Am. Chem. Soc.*, 2003, 125, 13940-13941.
40. T. Ahmada, I.A. Wania, N. Manzoorb, J. Ahmedc and A.M. Asiri, *Colloid Surf. B*, 107 (2013) 227-234.
41. N.S. Shaligram, M. Bule, R. Bhambure, R.S. Singhal, S.K. Singh, G. Szakacs and A. Pandey, *Process Biochem.*, 44 (2009) 939-943.
42. M. Gajbhiye, J. Kesharwani, A. Ingle, A. Gade and M. Rai, *Nanomed. Nanotechnol. Biol. Med.*, 5 (2009) 382-386.
43. A. Gole, C. Dash, V. Ramachandran, A.B. Mandale, S.R. Sainkar, M. Rao and M. Sastry, *Langmuir*, 17 (2001) 1674-1679.
44. D.S. Balaji, S. Basavaraja, R. Deshpandeb, D.B. Maheshb, B.K. Prabhakara and A. Venkataraman, *Colloid Surf. B*, 68 (2009) 88-92.
45. Z. Jian, Z. Xiang and W. Yongchang, *Microelectron. Eng.*, 77 (2005) 58-62.
46. A. Mooradian, *Phys. Rev. Lett.*, 22 (1968) 185-187.
47. T. Huang and R.W. Murray, *J. Phys. Chem. B*, 105 (2001) 12498-12502.
48. R. Sankara, A. Karthik, A. Prabua, S. Karthik, K.S. Shivashangari and V. Ravikumar, *Colloids Surf. B*, 108 (2013) 80-84.
49. U. Suriyakalaa, J.J. Antony, S. Suganya, D. Siva, R. Sukirtha, S. Kamalakkannan, P.B.T. Pichiah and S. Achiraman, *Colloids Surf. B*, 102 (2009) 189-194.
50. S.E.W. Jones, F.W. Campbell, R. Baron, L. Xiao and R.G. Compton, *J. Phys. Chem. C*, 112 (2008) 17820-17827.
51. H.W. Cheng, S. Thiagarajan and S.M. Chen, *Int. J. Electrochem. Sci.*, 6 (2011) 4150-4163.
52. A. Balamurugan, K.C. Ho, S.M. Chen and T.Y. Huang, *Colloids Surf. A*, 362 (2010) 1-7.
53. Y. Li, S.M. Chen, M.A. Ali and F.M.A. AlHemaid, *Int. J. Electrochem. Sci.*, 8 (2013) 2691-2701.
54. M. Giovanni and M. Pumera, *Electroanalysis*, 24 (2012) 615-617.